THE JOURNAL OF BIOLOGICAL CHEMISTRY VOL. 290, NO. 43, pp. 26270–26281, October 23, 2015

Akt Pathway Activation by Human T-cell Leukemia Virus Type 1 Tax Oncoprotein*

Received for publication, August 12, 2015 Published, JBC Papers in Press, August 31, 2015, DOI 10.1074/jbc.M115.684746

Mathew A. Cherian[‡], Hicham H. Baydoun[‡], Jacob Al-Saleem[§¶], Nikoloz Shkriabai[§‖], Mamuka Kvaratskhelia[§‖], Patrick Green[§¶], and Lee Ratner[‡1]

From the [‡]Division of Oncology, Department of Medicine, Washington University School of Medicine, St. Louis, Missouri 63110 and the [§]Center for Retrovirus Research and Departments of [‖]Pharmaceutics and Pharmaceutical Chemistry and [¶]Veterinary Biosciences, The Ohio State University, Columbus, Ohio 43210

Background: HTLV-1, not HTLV-2, is leukemogenic, and its oncoprotein, Tax1, includes a PDZ domain-binding motif (PBM).
Results: Tax1 induces Akt phosphorylation dependent on the PBM, which is overcome by membrane expression of PTEN and PHLPP.
Conclusion: Tax1 inhibits PI3K-Akt regulatory phosphatases.
Significance: Akt activation may contribute to the leukemic potential of HTLV-1 and provides a new therapeutic target.

Human T-cell leukemia virus (HTLV) type 1, the etiological agent of adult T-cell leukemia, expresses the viral oncoprotein Tax1. In contrast, HTLV-2, which expresses Tax2, is non-leukemogenic. One difference between these homologous proteins is the presence of a C-terminal PDZ domain-binding motif (PBM) in Tax1, previously reported to be important for non-canonical NFκB activation. In contrast, this study finds no defect in non-canonical NFκB activity by deletion of the Tax1 PBM. Instead, Tax1 PBM was found to be important for Akt activation. Tax1 attenuates the effects of negative regulators of the PI3K-Akt-mammalian target of rapamycin pathway, phosphatase and tensin homologue (PTEN), and PHLPP. Tax1 competes with PTEN for binding to DLG-1, unlike a PBM deletion mutant of Tax1. Forced membrane expression of PTEN or PHLPP overcame the effects of Tax1, as measured by levels of Akt phosphorylation, and rates of Akt dephosphorylation. The current findings suggest that Akt activation may explain the differences in transforming activity of HTLV-1 and -2.

Human T-cell leukemia virus (HTLV)[2] type 1 is the etiological agent of adult T-cell leukemia (ATL) (1, 2). ATL, in its acute form, which includes the majority of cases, is an aggressive T-cell malignancy. Median survival is measured in months despite aggressive management with modern multiagent chemotherapy regimens.

The integrated HTLV-1 genome expresses a 40-kDa protein, Tax1, that, when expressed in isolation, reproduces many of the transformative properties of the virus (3). Tax1 induces anchorage independence and loss of contact inhibition when expressed in fibroblasts, and these cells form tumors in nude mice (4). Tax1 is leukemogenic in transgenic mice (5).

Tax1 activates a number of oncogenic pathways, including the canonical NFκB, cAMP-response element-binding protein/activating transcription factor, and serum response factor pathways (6, 7). Canonical NFκB signaling occurs when IKKβ is activated by upstream serine threonine kinases, causing IκBα and IκBβ phosphorylation, ubiquitination, and degradation, and releasing heterodimers of p50 with RelA or c-Rel to translocate to the nucleus. IKKγ is an adaptor between IKKβ and upstream kinases, and it is a Tax1-interactive protein. Previous studies demonstrated that activation of the canonical NFκB pathway is critical for Tax1 immortalization of peripheral blood lymphocytes (8).

HTLV-2 is a non-leukemogenic strain of HTLV (9). HTLV-2 Tax (Tax2) has lower transforming activity than Tax1 (7, 10–16). Tax2 induces canonical NFκB activation equal to that of Tax1 (8, 10), but Tax2 induction of non-canonical NFκB is weaker than that of Tax1 (12). The non-canonical pathway involves activation of IKKα, and phosphorylation of NFκB2/p100, resulting in proteolytic processing to p52.

Two determinants of Tax1 for non-canonical NFκB activation were identified, a leucine zipper-like region (LZ; amino acids 225–232) and a C-terminal PDZ domain-binding motif (PBM; amino acids 350–353), both missing from Tax2 (17). Tax1 binds p100, acting as a bridge with IKKγ (18). The role of

* This work was supported, in whole or in part, by National Institutes of Health Grants CA94056, CA100730, and CA63413 and Grant T32 HL07088 (to M. C.). This work was also supported by Lymphoma and Leukemia Foundation Grant LLS6067-10, American Society of Hematology Research Training Award for Fellows, and Lymphoma Research Foundation Grant LRF307181203 (to H. B.). The authors declare that they have no conflicts of interest with the contents of this article.

[1] To whom correspondence should be addressed: Dept. of Medicine, Washington University School of Medicine, 660 S. Euclid Ave., Box 8069, St. Louis, MO 63110. Tel.: 314-362-8836; Fax: 314-727-2120; E-mail: lratner@dom.wustl.edu.

[2] The abbreviations used are: HTLV, human T-cell leukemia virus; Akt, protein kinase B; ATL, adult T-cell leukemia; GSK, glycogen synthase kinase; hScrib, *Drosophila* scribbled homolog/Vartul; IKK, inhibitor of κB kinase; LZ, leucine zipper region; mTOR, mammalian target of rapamycin; Myr, myristic acid; MAGI, membrane-associated guanylate kinase inverted; NFκB, nuclear factor of the κ light chain enhancer of activated B-cell; PBM, PDZ domain-binding motif; PBMC, peripheral blood mononuclear cell; PDZ, post-synaptic density/discs large/zona occludens protein; PHLPP, PH domain and leucine-rich repeat protein phosphatase; PIP_3, phosphatidylinositol 3,4,5-trisphosphate; PTEN, phosphatase and tensin homologue; RPMI medium, Roswell Park Memorial Institute medium; Tax, HTLV viral transactivator; Tet, tetracycline; TSC2, tuberous sclerosis 2.

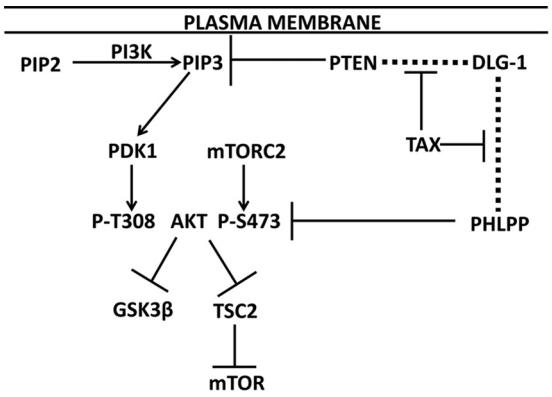

FIGURE 1. **Role of PTEN and PHLPP in PI3K-Akt activation and potential role of Tax1.** The plasma membrane is shown at the top of the figure, the site of phosphatidylinositol 4,5-bisphosphate (*PIP2*) conversion to PIP_3, and DLG-1 PDZ domain binding to PTEN and PHLPP (indicated by *dashed lines*). PIP_3 activation of PDK1 resulting in phosphorylation of Akt at Thr-308 and mTORC2 phosphorylation of Ser-473 are shown. PTEN is a PIP_3 phosphatase, and PHLPP is a P-AktSer-473 (*P-AktS473*) phosphatase. Activated Akt promotes phosphorylation and inhibition of GSK3β and TSC2; the latter effect results in mTOR activation. This study tests the hypothesis that Tax1 inhibits PTEN and PHLPP binding to DLG-1, thereby diminishing their phosphatase activities for PIP_3 and Akt, respectively.

the Tax1 LZ and PBM domains in non-canonical NFκB activation is unclear, because neither domain is required for the binding of Tax1 to p100 (12, 13).

PDZ domain proteins include scaffolding proteins, such as DLG-1, hScrib, MAGI-1, and NHERF1, which bind to the C-terminal PBMs of integral membrane proteins. PDZ domain proteins can then bind cytoplasmic proteins, such as PTEN and PHLPP (PH domain and leucine-rich repeat protein phosphatase), key phosphatases that negatively regulate the PI3K-Akt-mTOR pathway (Fig. 1) (19–23). PTEN dephosphorylates phosphatidylinositol 3,4,5-trisphosphate (PIP_3), restraining PDK1 and TORC2 phosphorylation at residues Thr-308 and Ser-473 of Akt. PHLPP dephosphorylates AktSer-473 (24). Phosphorylated Akt phosphorylates and inhibits GSK3β, as well as TSC1 and -2, to activate mTOR (21).

Tax1 binds to PDZ domain proteins, including DLG-1, hScrib, MAGI-1, and MAGI-3, via its C-terminal PBM (25–28). Given that Tax1, PTEN, and PHLPP bind to common PDZ proteins, and these interactions enhance PTEN- and PHLPP-mediated negative regulation of the PI3K-Akt pathway (20, 22), we investigated whether Tax1 competes for binding to these proteins to induce Akt pathway activation.

Materials and Methods

Cell Culture—Tet-On Tax1 Jurkat cells, obtained from Edward Harhaj, The Johns Hopkins University, were originally made by Warner Greene, University of California at San Francisco (29). Jurkat, 293T, Hut102, and MT4 cells were obtained from American Type Tissue Collection. Cell lines were maintained at 37 °C and 5% CO_2 in complete media supplemented with 10% fetal bovine serum, 4 mM L-glutamine, 100 units/ml penicillin, 100 μg/ml streptomycin, and 0.25 μg/ml amphotericin B. T-cell lines, including Jurkat, MT4, and Hut102 cells were maintained in complete RPMI 1640 medium (cRPMI). 293T cells were maintained in complete DMEM with 1 mM sodium pyruvate. Tet-On Tax1 Jurkat cells were expanded in cRPMI 1640 medium with tetracycline-free fetal bovine serum (Clontech). For induction, these cells were cultured in cRPMI 1640 medium with 1 μg/ml doxycycline for 48 h. For CD3/CD28 stimulation experiments, preservative-free anti-CD3 (clone OKT3) and anti-CD28 (clone ANC28) at 1 μg/ml in PBS were bound to tissue culture-treated polystyrene plates by incubation overnight. Plates were then blocked for 30 min with cRPMI 1640 medium prior to application of cells. Pan-PI3K inhibitors Ly294002 and Akt inhibitor MK2206 were obtained from Selleckchem. For dephosphorylation assays, cells were treated with either 50 μM Ly294002 or 1 μM MK2206.

Transfections—Jurkat cells were transiently transfected with 0.1 μg/μl DNA by electroporation in 0.4-mm cuvettes suspended in 150 μl of cRPMI 1640 medium with 5% serum at 340 V, 350-microfarad capacitance, and 750 ohms using a BTX ECM 600 exponential decay electroporator. 293T cells were transiently transfected with TransIT (Mirus Bio) or by electroporation at 220 V, 350 microfarad capacitance, and 750 ohms.

Plasmids expressing Tax1, Tax2, and the C-terminal PBM deletion mutant of Tax1 (Tax1ΔPBM) were amplified by PCR from the HTLV-1 molecular clone (pACH) and HTLV-2 molecular clone (pH6neo), respectively. The Tax1 LZ region (amino acids 225–232) mutant (Tax1ΔLZ) was made by overlap extension of PCR fragments corresponding to nucleotides 1–672 of *tax1*, an oligonucleotide corresponding to nucleotides 673–697 of *tax2*, and the PCR fragment of nucleotides 699–1059 of *tax1*, each with the corresponding additional overlap sequences. Thus, the corresponding region of Tax2 replaces the LZ region of Tax1 in the Tax1ΔLZ mutant. NheI and XmaI sites were introduced during PCR. The PCR products were digested with NheI and XmaI and cloned into the corresponding sites of the backbone vector TriExNeo creating S-tagged and polyhistidine-tagged expression constructs of the respective proteins. Protein expression was confirmed by Western blot, and biological activity was confirmed by co-transfection with a luciferase reporter plasmid that is driven by the HTLV-1 long terminal repeat promoter-enhancer.

The HA-tagged PTEN expression vector (800 pSG5L HA-PTEN WT), originally made by W. R. Sellers (Harvard University), was obtained from Addgene (plasmid no. 10750) (30). PTEN expression constructs with an N-terminal myristoylation acceptor sequence derived from v-Src, leading to constitutive membrane localization, has been previously described (MyrPTEN) (31). The MyrPTEN expression vector, 1006 pSG5L HA-MyrPTEN, made by W. R. Sellers, was obtained from Addgene (plasmid no. 10776).

The HA-tagged PHLPP1α expression vector (pcDNA3 PHLPP1) was a gift from Tianyan Gao, University of Kentucky (24). Constitutive membrane localization of PHLPP, using an N-terminal myristoylation sequence derived from v-Src, was described previously (20). The HA-PHLPP1α coding sequence was ligated in place of HA-PTEN in the pSG5L Myr-HA-PTEN expression plasmid. pEGFP SAP97β (GFP-DLG1), a gift from J. Miner, Washington University, was originally made by W. Green, University of Chicago (32).

PAGE and Western Blotting—Cells were lysed in Tris-HCl, pH 6.8, with 2% SDS, 2% Igepal CA630, 10 mM sodium β-glycerophosphate, 10 mM sodium fluoride, 2.5 mM sodium pyro-

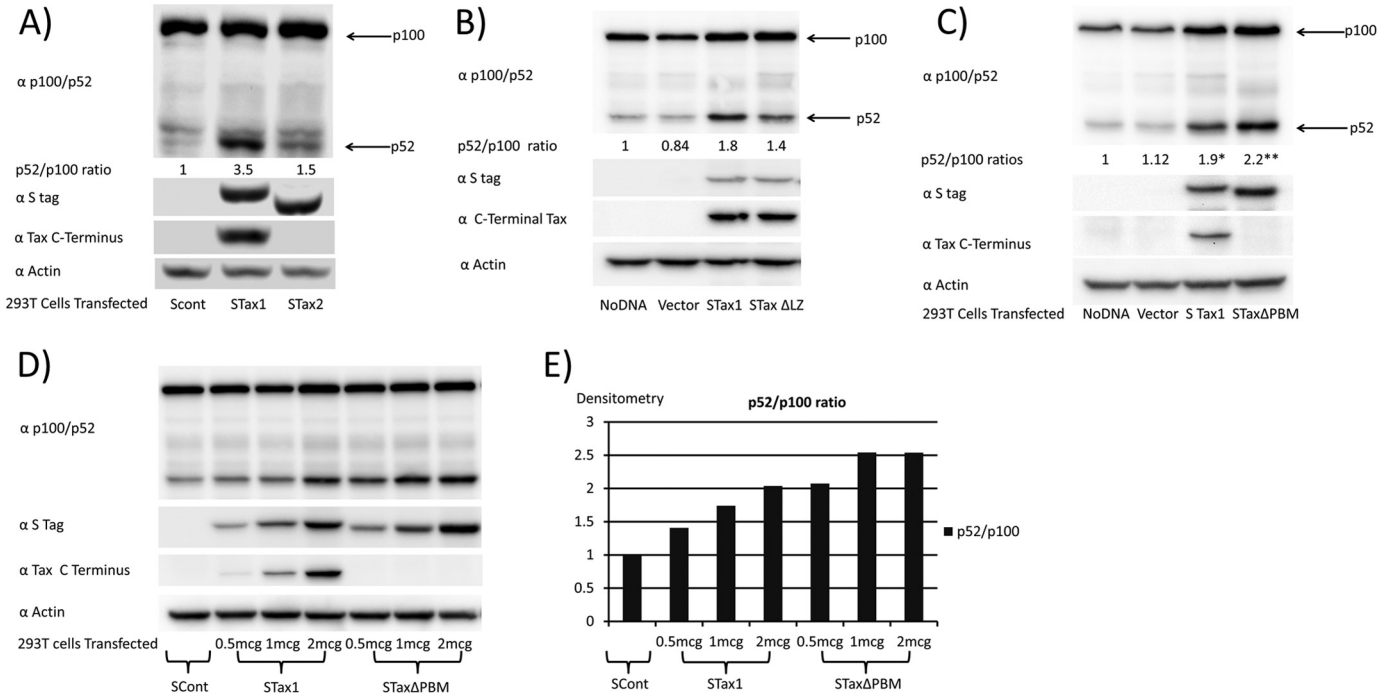

FIGURE 2. **Tax1 activates the alternative NFκB pathway.** *A,* 293T cells were transiently transfected with empty vector (*SCont*), S-tagged Tax1 (*STax1*), or S-tagged Tax2 (*STax2*) expression plasmids. Activation of the non-canonical NFκB pathway was measured by processing of p100 (NFκB2) to p52, as assessed by immunoblot for p52/p100, and quantified by densitometry. Immunoblots were also performed with antibody to S tag, an antibody to Tax1 that recognizes a C-terminal epitope, and antibody to actin. *B,* p100 processing in untransfected 293T cells, and cells transiently transfected with empty vector or expression plasmids for S-tagged Tax1 or S-tagged leucine zipper-like region mutant (amino acids 225–232) of Tax1. *C,* p100 processing in untransfected 293T cells, and cells transiently transfected with empty vector or expression vectors for STax1 or S-tagged TaxΔPBM of Tax1. *D,* p100 processing in 293T cells transiently transfected with vector and increasing amounts of STax1 or STaxΔPBM. *E,* dose response of p100 processing with increasing expressions of STax1 or STaxΔPBM. Experiments corresponding to *A–C* were repeated twice each.

phosphate, 1 mM sodium orthovanadate, and EDTA-free protease inhibitor mixture (Roche Applied Science). Lysates were sonicated on ice for 20 s. Protein quantification was performed using the bicinchoninic acid assay (33). Equal amounts of protein (20–40 μg) were loaded onto polyacrylamide gels, and electrophoresis was performed according to standard methods described by Ornstein (34) and modified by Laemmli (35). Primary antibodies were diluted in 5% protease-free bovine serum albumin and secondary antibodies in 10% skimmed milk. Blots were imaged by enhanced chemiluminescence using a Chemi-Doc imager (Bio-Rad) and quantified using the Bio-Rad proprietary software.

The following antibodies were used for Western blots. Rabbit primary antibodies to P-AktSer-473, P-AktThr-308, total Akt, P-GSK3βSer-9, PTEN, and HA tag were obtained from Cell Signaling Technologies. Rabbit antibody to PHLPP was obtained from Abcam. Rabbit anti-GFP antibody was obtained from Clontech. Mouse primary antibodies to NFκB2/p100 and S tag were obtained from Millipore. Hybridoma 1316 for Tax1 was obtained from the AIDS Repository, National Institutes of Health.

Co-immunoprecipitation—293T cells were lysed in buffer consisting of phosphate-buffered saline (PBS) with 10% glycerol, 1% Igepal CA 630, 0.1% sodium deoxycholate, 10 mM sodium β glycerophosphate, 10 mM sodium fluoride, and 2.5 mM sodium pyrophosphate with protease inhibitor cocktail. Immunoprecipitation was performed with goat anti-GFP antibody (Genetex) using protein A/G-conjugated cross-linked agarose beads. Following overnight incubation of lysates with immunoglobulin and beads, the beads were washed with PBS with 0.1% sodium deoxycholate five times, and then protein was eluted by incubation at 70 °C for 10 min in 1× SDS sample buffer.

Proteomics—Lysates from 293T cells transfected with S-Control, STax1, and STaxΔPBM expression plasmids were subjected to tandem affinity purification with nickel beads followed by anti S tag antibody with protein-A/G beads. Eluted proteins were subjected to trypsin digestion, and peptide fragments were separated by capillary-liquid chromatography followed by peptide sequencing by tandem mass spectrometry (MS/MS) using a Thermo Finnigan LTQ Orbitrap mass spectrometer equipped with a microspray source (Michrom Bioresources) (36).

Statistics—Densitometry was analyzed by one-tailed Student's *t* test for statistical significance.

Results

HTLV-1 Tax Promotes p100 (NFκB2) Processing—Previous studies suggested that Tax1 but not Tax2 promotes p100 processing. To confirm these findings with S-tagged Tax proteins, 293T cells were transfected with control vector (SCont), or expression plasmids for S-tagged Tax1 (STax1), or S-tagged Tax2 (STax2) (Fig. 2*A*). After 48 h, cells were lysed and immunoblots were performed with an antibody that recognizes p100, and the p52 processed product (α p100/p52). As compared with the SCont-transfected cells, the ratio of protein levels, p52/

p100, was 3.5 for STax1-expressing cells and 1.5 for STax2-expressing cells. In this experiment, there were no significant differences in the levels of expression of STax1 and STax2 proteins, as measured with an antibody to STag (αS tag), or levels of protein loading on the gel, as shown with an antibody to actin. An antibody to the C terminus of Tax1 demonstrated reactivity to STax1 but not STax2.

Two determinants of Tax1 were previously proposed to be required for non-canonical NFκB activation, an LZ region (amino acids 225–232) and a PBM (amino acids 350–353). Both of these domains are present in Tax1 but not Tax2 (17). To further examine this claim, we made S-tagged Tax1 plasmids expressing mutants with the leucine zipper-like region exchanged for the corresponding region of Tax2 or deletion of the C-terminal PBM. Transfection of 293T cells with the plasmid expressing the leucine zipper mutant of Tax1 (STax1ΔLZ) resulted in a partial defect in p100 processing to p52, as compared with wild-type Tax1 (STax1; $p = 0.02$; Fig. 2*B*). Surprisingly, when we tested the PBM deletion mutant of Tax1 (Tax1ΔPBM), we did not see defective p100 processing to p52 (Fig. 2*C*). In fact, p100 processing was significantly increased with expression of Tax1ΔPBM as compared with Tax1 ($p = 0.01$). Dose-response experiments were also performed with wild-type Tax1 and Tax1ΔPBM (Fig. 2, *D* and *E*). At both low and high levels of expression of Tax1 and Tax1ΔPBM, Tax1 and the ΔPBM mutant were found to be capable of inducing p100 processing to p52. Tax1ΔPBM is therefore not defective in inducing p100 processing when compared with Tax1.

Tax1, but Not the PBM Deletion Mutant of Tax1, Activates Akt—Although differences were not found in non-canonical NFκB activation in the comparison of Tax1 to Tax1ΔPBM, Tax1ΔPBM is attenuated in its ability to transform cells (10, 37). We therefore sought alternative explanations for the difference in transformation potency.

Previous studies showed that PTEN bound DLG-1 (21, 23). Moreover, previous work also suggested that the Tax1 PDZ-binding motif mediated interaction with several cellular proteins, including DLG-1 (25). To verify these findings, proteins interacting with STax1 or STax2 in transfected 293T cells were co-purified by immunoaffinity chromatography and subjected to MS/MS analysis. Seven unique peptides derived from DLG-1 and 22 unique peptides from hScrib were identified in STax1 but not STax2 or STax1ΔPBM complexes (Fig. 3).

Because the C terminus of Tax1, PTEN, and PHLPP bind to common PDZ proteins, and these interactions of PTEN and PHLPP enhance their negative regulation of the PI3K-Akt-mTOR pathway, we hypothesized that Tax1 may activate Akt by competing with PTEN and PHLPP for binding to PDZ proteins and displacing these phosphatases from sites of PIP_3 synthesis at the plasma membrane.

The level of Akt activation in HTLV-1 transformed cell lines Hut102 and MT4 was compared with IL-2/phytohemagglutinin-activated PBMCs (Fig. 4*A*). HTLV-1 transformed Tax-positive cell lines showed a higher level of phospho-Akt (P-AktSer-473) and downstream phosphoglycogen synthase kinase 3 (P-GSK3βSer-9). PTEN and PHLPP expression were higher in the HTLV-1 transformed cell lines than PBMCs. In these cell lines, Tax1 is expressed as a 40-kDa protein or as a fusion protein with the envelope glycoprotein (Env-Tax), or both.

Effects on Akt activation were also examined in cells stably transfected with a Tax1 expression plasmid under the control of a doxycycline-regulated promoter (Fig. 4*B*). Levels of P-Akt-Thr-308, normalized to total Akt (P-AktThr-308/Akt) and P-AktSer-473/Akt were 13.5- and 6.3-fold greater (Fig. 4*B, lane 4/lane 1*), respectively, in doxycycline-treated Tet-On Tax1 cells as compared with doxycycline-treated Jurkat cells lacking the expression plasmid. Levels of P-AktThr-308/Akt and P-AktSer-473/Akt were 3.9- and 2.9-fold greater (Fig. 4*B, lane 7/lane 1*) in Tet-On Tax1 Jurkat cells in the absence of doxycycline, compared with control Jurkat cells in the presence of doxycycline. The low levels of Akt phosphorylation seen in the absence of doxycycline are presumably due to leakiness of the promoter (Fig. 4*B, lane 7*).

With CD3/CD28 stimulation, levels of P-AktThr-308/Akt and P-AktSer-473/Akt were induced 5.8- and 4.3-fold in Jurkat cells lacking Tax1 (Fig. 4*B, lane 3/lane 1*), 2.9- and 3.8-fold in Tet-On Tax1 Jurkat cells treated with doxycycline (Fig. 4*B, lane 6/lane 4*), and 19.4- and 8.3-fold, respectively (Fig. 4*B, lane 9/lane 7*), in Tet-On Tax1 Jurkat cells not treated with doxycycline. These findings suggest that Tax1 and T-cell receptor simulation have additive effects on Akt phosphorylation.

Levels of total Akt declined with Akt activation by Tax1 or CD3/CD28, consistent with activation-induced proteasome degradation, which has been previously reported (38, 39). Levels of GSK3β phosphorylation correlated with those of Akt phosphorylation, confirming constitutive phosphorylation of a downstream target in Tax1-expressing cells.

To determine whether the PDZ-binding domain of Tax1 is important for Akt phosphorylation, Jurkat cells were transfected with a control vector or plasmids expressing wild-type STax1, STax2, or STax1ΔPBM (Fig. 4*C*). The level of P-AktThr-308 was 1.93-fold higher in STax1-expressing than control Jurkat cells. In contrast, no increase in AktThr-308 phosphorylation was seen in STax2- or STax1ΔPBM-expressing cells compared with control Jurkat cells. It is likely that P-Akt levels are not as high as in Tet-On Tax1 Jurkat cells due to lower levels of expression of Tax1 in these transiently transfected cells. Results from four independent experiments revealed a statistically significant difference between P-AktThr-308/total Akt ratios in STax1-expressing *versus* STax1ΔPBM-expressing cells ($p = 0.033$) confirming the absence of Akt activation by STax1ΔPBM. This suggests that the C-terminal PBM of Tax1 is required for Akt activation.

To examine Akt phosphorylation in another cell type, 293T cells were transfected with a control vector or plasmids expressing wild-type STax1, STax2, or STax1ΔPBM (Fig. 4*D*). The level of P-AktThr-308 was 1.3-fold higher in STax1-expressing than control 293T cells. No increase in AktThr-308 phosphorylation was seen in STax2- or STax1ΔPBM-expressing cells. The apparent decrease in Akt phosphorylation seen with expression of STax2 and STax1ΔPBM may be due to indirect effects through IKK activation (40).

Forced Membrane Expression of PTEN Overcomes Effects of Tax1 on Akt Phosphorylation—To examine the role of PTEN in Tax-mediated Akt phosphorylation, the effect of exogenous

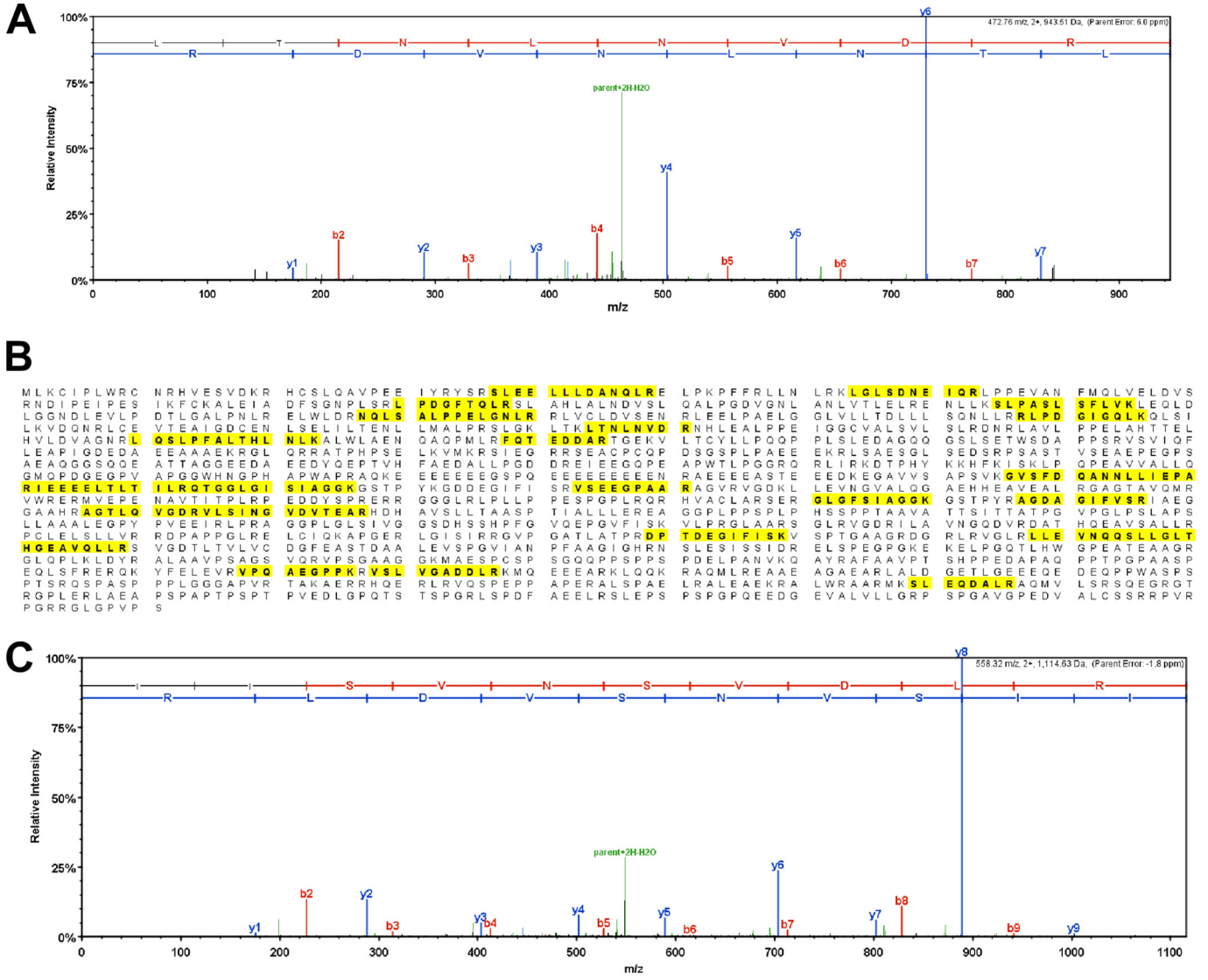

FIGURE 3. **MS/MS analysis to show hScrib and DLG-1 binding to STax1.** *A*, representative MS/MS data for one of the tryptic peptides (LTNLNVDR) from hScrib is shown. *B*, identified peptide sequences in hScrib are indicated in *bold* and highlighted in *yellow*. The amino acid sequence coverage was 15% (249/1631 amino acids) with 22 unique peptides and 47 total spectra being identified in fractions with STax1. No peptides from hScrib were detected in fractions with STax2 or STax1ΔPBM. *C*, representative MS/MS data for one of the tryptic peptides (IISVNSVDLR) from DLG-1 is shown. *D*, identified peptide sequences in DLG-1 are indicated in *bold* and highlighted in *yellow*. The amino acid sequence coverage was 12% (110/926 aa) with 7 unique peptides and 13 total spectra being identified in fractions with STax1. No peptides from DLG-1 were detected in fractions with STax2 or STax1ΔPBM.

expression of PTEN was examined in Jurkat cells, a T-cell line lacking PTEN (Fig. 5*A*). In comparison with PTEN expression alone, co-expression of STax1 with PTEN resulted in a significant increase of P-AktThr-308 levels ($p = 0.038$) (Fig. 5*B*). Statistical comparison of STax1 induction of P-AktThr-308 in the presence and absence of co-expressed PTEN revealed that co-expression of PTEN exaggerated P-AktThr-308 activation by Tax1 (mean 2.4 *versus* 1.7; $p = 0.027$).

An expression plasmid was used that encoded a form of PTEN with an N-terminal myristoylation acceptor motif (MyrPTEN, Fig. 5*C*). Myristoylation of PTEN has previously been shown to result in constitutive membrane association, compared with non-myristoylated PTEN (31). With MyrPTEN, expression of STax1 in Jurkat cells did not result in a significant increase in P-AktThr-308 ($p = 0.93$) or P-AktSer-473 ($p = 0.5$), as compared with cells lacking Tax1. This sug-

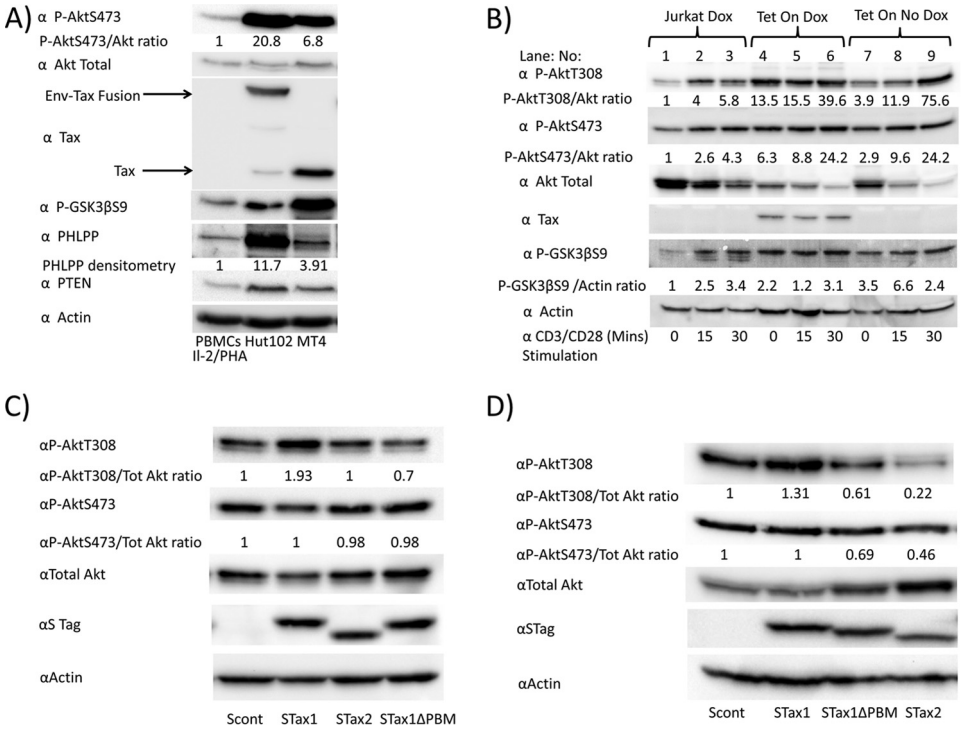

FIGURE 4. **Akt phosphorylation depends on the PDZ-binding domain of Tax1.** *A,* P-AktSer-473 (*P-AktS473*) and total Akt levels were determined in IL-2/phytohemagglutinin-stimulated PBMCs as compared with HTLV-1-immortalized cell lines Hut102 and MT4. The ratios of P-AktSer-473 to total Akt are shown as measured by densitometry. Immunoblots show the expression of Tax and Env-Tax fusion proteins in these cell lines, as well as GSK3β phosphorylation, and levels of PHLPP, PTEN, and actin. *B,* Jurkat cells and Tet-On Tax1 Jurkat cells were grown in the presence or absence of doxycycline (*Dox*) for 48 h and then stimulated for 0, 15, or 30 min on CD3/CD28-coated plates. *C,* Jurkat cells were transfected with empty vector or expression plasmids for STax1, STax2, or STax1ΔPBM. The ratios of P-AktThr-308 (*P-AktT308*) and P-AktSer-473 (*P-AktS473*) to total Akt are shown as measured by densitometry. Combined results of four separate experiments revealed statistically significant differences between P-AktThr-308/total Akt ratio for Jurkat cells expressing STax1 *versus* STax1ΔPBM ($p = 0.033$). *D,* 293T cells were transfected with empty vector or expression plasmids for STax1, STax1ΔPBM, or STax2. The ratios of P-AktThr-308 and P-AktSer-473 to total Akt are shown as measured by densitometry.

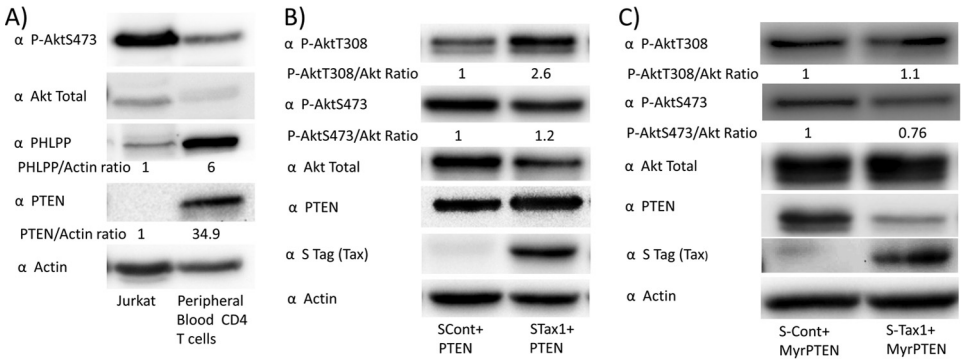

FIGURE 5. **Expression of membrane-associated PTEN overcomes the effects of Tax1 on levels of phosphorylated Akt.** *A,* expression of PTEN and PHLPP in Jurkat cells was compared with negatively selected peripheral blood $CD4^+$ T-cells. *B,* Jurkat cells were co-transfected with a plasmid expressing wild-type PTEN and with empty vector or STax1 expression plasmid. Levels of P-AktThr-308 (*P-AktT308*), P-AktSer-473 (*P-AktS473*), and total Akt were determined by immunoblot, and ratios were determined as described previously. Levels of PTEN and actin were also monitored by immunoblot. Statistical comparison of P-AktThr-308/total Akt ratios in four experiments of empty vector *versus* STax1 and two experiments of empty vector *versus* STax1 in the presence of co-transfected PTEN revealed a statistically significant increase in Tax1-induced P-AktThr-308 in the presence of PTEN *versus* the absence of PTEN ($p = 0.027$). *C,* Jurkat cells were transfected with an expression vector for myristoylated PTEN for constitutive membrane association, together with empty vector or STax1 expression vector. Experiments corresponding to *B* and *C* were repeated twice each.

gests that Tax1-induced Akt activation is due to decreased membrane localization of PTEN.

Dephosphorylation studies were performed to determine whether Tax1 expression diminished rates of Akt dephosphorylation. For this purpose, doxycycline-treated Jurkat or Tet-On Tax1 Jurkat cells were treated with a PI3K inhibitor, Ly294002 for 0, 10, 20, or 30 min, to shut off upstream signals (Fig. 6, *A* and *B*). Immunoblots were performed to determine P-AktThr-308 and P-AktSer-473 levels. The basal level of P-GSK3βSer-9 was increased 1.4-fold in Tet-On Tax1 Jurkat cells as compared with Jurkat cells. Levels of HSP90 and actin demonstrate equivalent protein loading for each sample. The rate of P-AktSer-473 dephosphorylation was significantly lower ($p < 0.0001$) in Tet-On Tax1 Jurkat cells than control Jurkat cells, indicating decreased phosphatase activity downstream of PI3K in Tax1-expressing cells.

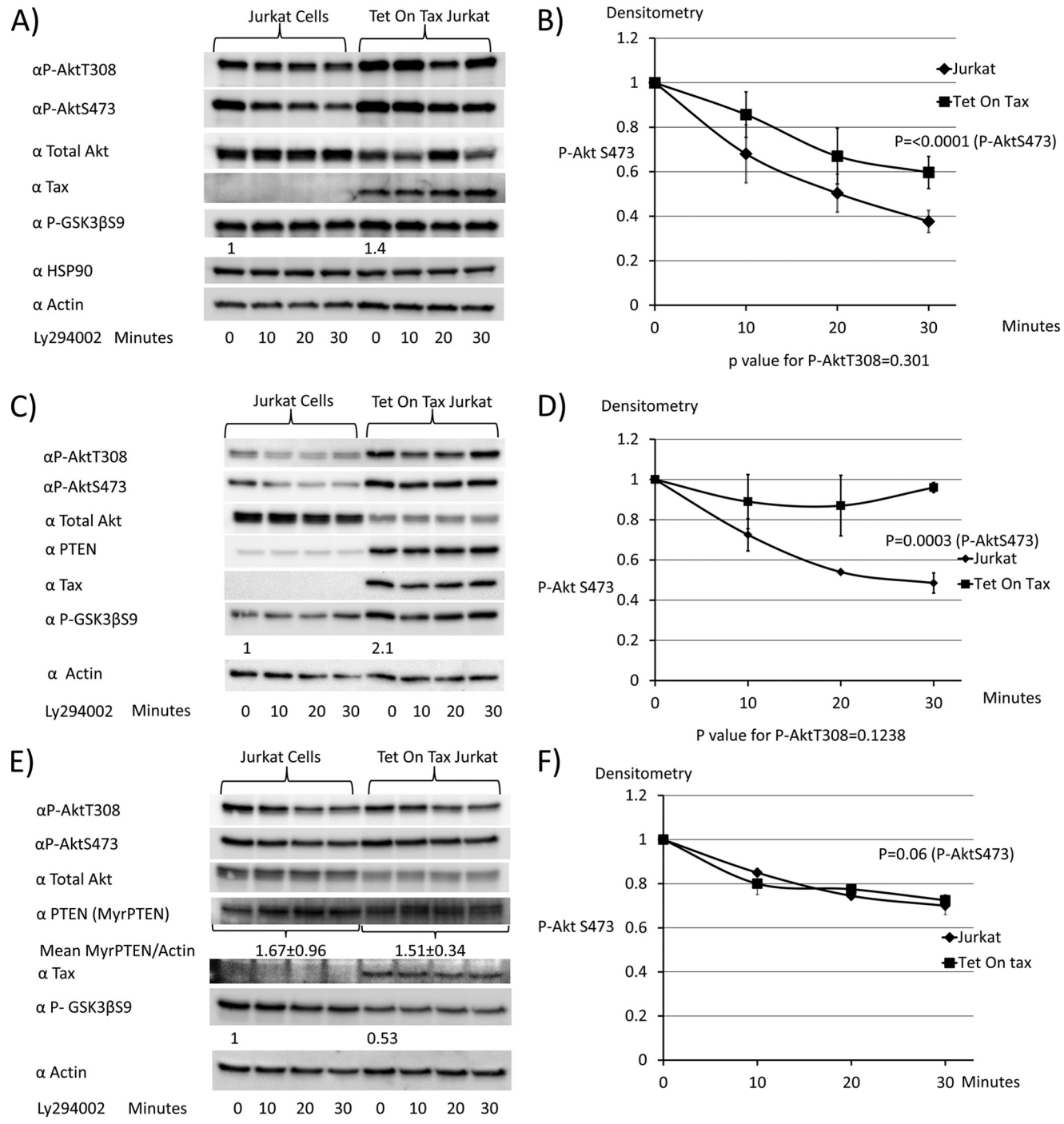

FIGURE 6. **Expression of membrane-associated PTEN overcomes the effects of Tax1 on rates of Akt dephosphorylation.** *A* and *B,* Jurkat cells and Tet-On Tax1 Jurkat cells maintained in doxycycline for 48 h were treated with the pan-PI3K inhibitor Ly294002, and samples were taken at serial time points to assess levels of P-AktThr-308 (*P-AktT308*) and P-AktSer-473(*P-AktS473*). Levels of Akt, Tax1, P-GSK3*β*, HSP90, and actin were examined by immunoblot. The level of P-AktSer-473 at each time point was normalized to values obtained at 0 min of Ly294002 treatment. *C* and *D,* doxycycline-treated Jurkat cells and Tet-On Tax Jurkat cells were transiently transfected for 6½ h with a wild-type PTEN expression plasmid and then treated with the pan-PI3K inhibitor Ly294002. Samples were taken at serial time points to compare Akt dephosphorylation rates as described above. *E* and *F,* doxycycline-treated Jurkat cells and Tet-On Tax1 Jurkat cells were transiently transfected with a myristoylated PTEN expression plasmid for 6½ h, treated with the pan-PI3K inhibitor Ly294002, and samples taken at serial time points to compare Akt dephosphorylation rates, as described above. Dephosphorylation curves were generated from two independent experiments in each case. The baseline P-AktSer-473 level is normalized to 1 for dephosphorylation curves.

Akt dephosphorylation kinetics were also examined in Jurkat and Tet-On Tax1 Jurkat cells transfected with an expression plasmid for PTEN (Fig. 6, *C* and *D*). Similar to the results in the absence of PTEN, expression of Tax1 inhibited dephosphorylation of P-AktSer-473 ($p = 0.0003$). P-GSK3*β*Ser-9 levels were increased 2.1-fold in Tax1-expressing cells as compared with control cells at time 0.

Akt dephosphorylation kinetics were next examined in Jurkat and Tet-On Tax1 Jurkat cells transfected with an expression plasmid for MyrPTEN (Fig. 6, *E* and *F*). Levels of MyrPTEN

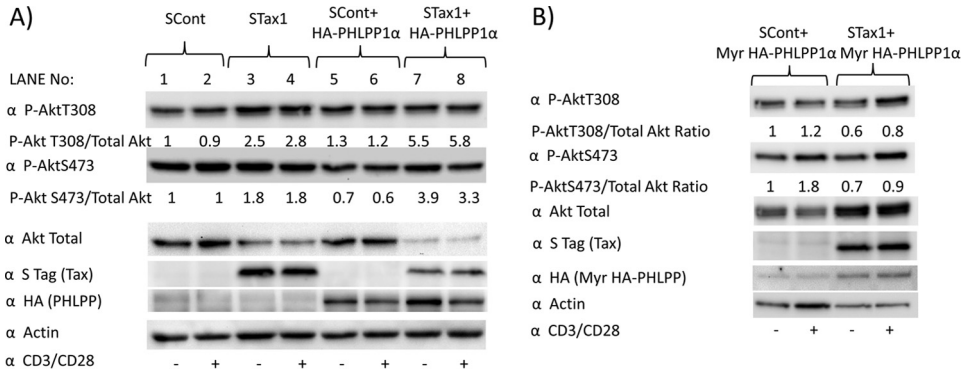

FIGURE 7. **Membrane expression of PHLPP overcomes the effects of Tax1 on Akt phosphorylation.** *A,* Jurkat cells were transfected with vector or STax1 expression plasmid with or without co-transfection of a PHLPP expression plasmid and then stimulated for 30 min on plates coated with or without CD3/CD28. Immunoblots were performed to assess level of P-AktThr-308 (*P-AktT308*), P-AktSer-473(*P-AktS473*), total Akt, Tax1, PHLPP, and actin. The ratios of P-AktSer-473 to total Akt were determined by densitometry. The ratio of Tax1-induced increase of P-AktThr-308/total Akt ratio with co-transfected PHLPP *versus* without transfected PHLPP is 1.69. The corresponding ratio for P-AktSer-473 is 3.1. *B,* Jurkat cells were co-transfected with a myristoylated PHLPP expression plasmid and empty vector or STax1 expression plasmid and stimulated for 30 min on plates coated with or without CD3/CD28. Experiments were repeated twice each.

were similar in both cell types. In the presence of MyrPTEN, rates of P-AktThr-308 and P-AktSer-473 dephosphorylation were indistinguishable in Jurkat and Tet-On Tax1 Jurkat cells. The P-GSK3βSer-9 level was higher by 1.9-fold in the control cells with expression of MyrPTEN, as compared with Tax1-expressing cells (Fig. 6*E*, *lane 5/lane 1*).

Forced Membrane Expression of PHLPP Overcomes Effects of Tax1 on Akt Phosphorylation—Jurkat cells have low levels of PHLPP, as compared with peripheral blood $CD4^+$ T-cells (Fig. 5*A*). Therefore, the effects of Tax1 on Akt phosphorylation were examined in Jurkat cells with or without exogenous PHLPP expression (HA-PHLPP1α, Fig. 7*A*). Ratios of P-Akt-Thr-308 and P-AktSer-473 to total Akt were 4.2- and 5.6-fold higher, respectively, in HA-PHLPP-expressing cells in the presence compared with the absence of Tax1 (Fig 7*A*, *lane 7*/*lane 5*). Co-expression of PHLPP exaggerated Tax1-induced Akt activation; P-AktThr-308/total Akt ratio with co-transfected PHLPP *versus* without PHLPP co-transfection was 1.69 and the corresponding ratio for P-AktSer-473 was 3.1 (Fig 7*A* (*lane 7* ÷ *lane 5*)/(*lane 3* ÷ *lane 1*)) The decline in total Akt levels with activation is consistent with activation-induced degradation, which has been previously described (38, 39).

Forced membrane expression of PHLPP using an N-terminal myristoylation sequence has been previously described (20). In the presence of MyrHA-PHLPP, the ratios of P-AktThr-308 and P-AktSer-473 to total Akt were similar in the presence of Tax1 to that in the absence of Tax1 ($p = 0.75$) (Fig. 7*B*). This suggests that Tax1-induced Akt activation is also due to decreased membrane localization of PHLPP, as it is reversed by forced membrane localization of PHLPP. The increase in total Akt in Tax1-expressing cells as compared with control cells may be due to transcriptional effects of Tax1 on Akt expression, which are unmasked in the absence of concomitant activation-induced Akt degradation.

Akt dephosphorylation studies were also measured after treatment of Jurkat cells for 0, 5, 10, or 15 min with MK2206, an Akt inhibitor. Rates of dephosphorylation with MK2206 were more rapid than with the PI3K inhibitor Ly294002, given that MK2206 is a direct Akt inhibitor, and therefore the effects on Akt dephosphorylation are immediate. In addition, rates of dephosphorylation of Akt on exposure to PI3K inhibitors in PTEN-mutated cell lines, such as Jurkat cells, is likely delayed due to a slower conversion of PIP_3 to phosphatidylinositol 4,5-bisphosphate, because PTEN is a phosphatidylinositol 3-phosphate phosphatase.

The rates of dephosphorylation of P-AktThr-308 ($p = 0.004$), P-AktSer-473 ($p = 0.0002$), and downstream P-GSK3βSer-9 were lower in Tet-On Tax1 Jurkat cells than control Jurkat cells (Fig. 8, *A* and *B*). This suggests that an Akt phosphatase is inhibited by Tax1. Similar results were obtained in the presence of exogenous expression of HA-PHLPP (Fig. 8, *C* and *D*) ($p = 0.02$ for P-AktThr-308 and P-Ser-473 dephosphorylation). However, in the presence of Myr HA-PHLPP, rates of Akt dephosphorylation were greater in the presence than the absence of Tax1 (Fig. 8, *E* and *F*) ($p = 0.014$ for P-AktThr-308 and $p = 0.0175$ for P-AktSer-473). In addition, levels of P-GSK3βSer-9 at time 0 were significantly higher in the control Jurkat cells than in the Tet-On Tax1 Jurkat cells ($p = 0.04$).

Tax1 Attenuates Binding of PTEN to DLG-1—To determine whether Tax1 competes with PTEN for interaction with DLG-1, co-immunoprecipitation assays were performed in 293T cells (Fig. 9). Immunoprecipitates with control IgG, using lysates of cells expressing DLG-1 (GFP-DLG-1), PTEN, and Tax1 (STax1) or Tax1ΔPBM (STax1ΔPBM) did not show reactivity with antibodies to PTEN, S tag, or GFP (Fig. 9*A*, *lanes 1* and *2*).

Expression of Tax1 with PTEN demonstrated Tax1 in complex with DLG-1 but less PTEN associated with DLG-1 than in the absence of Tax1 (Fig. 9*A*, *lane 5* and *4*). In contrast, expression of Tax1ΔPBM with PTEN showed no interaction of Tax1ΔPBM with DLG-1 (Fig. 9*A*, *lane 6*), and similar levels of PTEN were associated with DLG-1 to that seen in the absence of Tax1 (Fig. 9*A*, *lanes 4* and *6*). Immunoblots of total lysates for PTEN, Stag, and GFP-DLG-1 confirmed the expression of these proteins in the expected lanes (Fig. 9*A*, *bottom three panels*). Somewhat higher levels of PTEN and DLG-1 expression in the presence of Tax1 or Tax1ΔPBM than in their absence are likely due to trans-activation effects of Tax1 on the promoters used in these expression plasmids (Fig. 9*A*, *lanes 3* and *4 versus lanes 1, 2, 5,* and *6*).

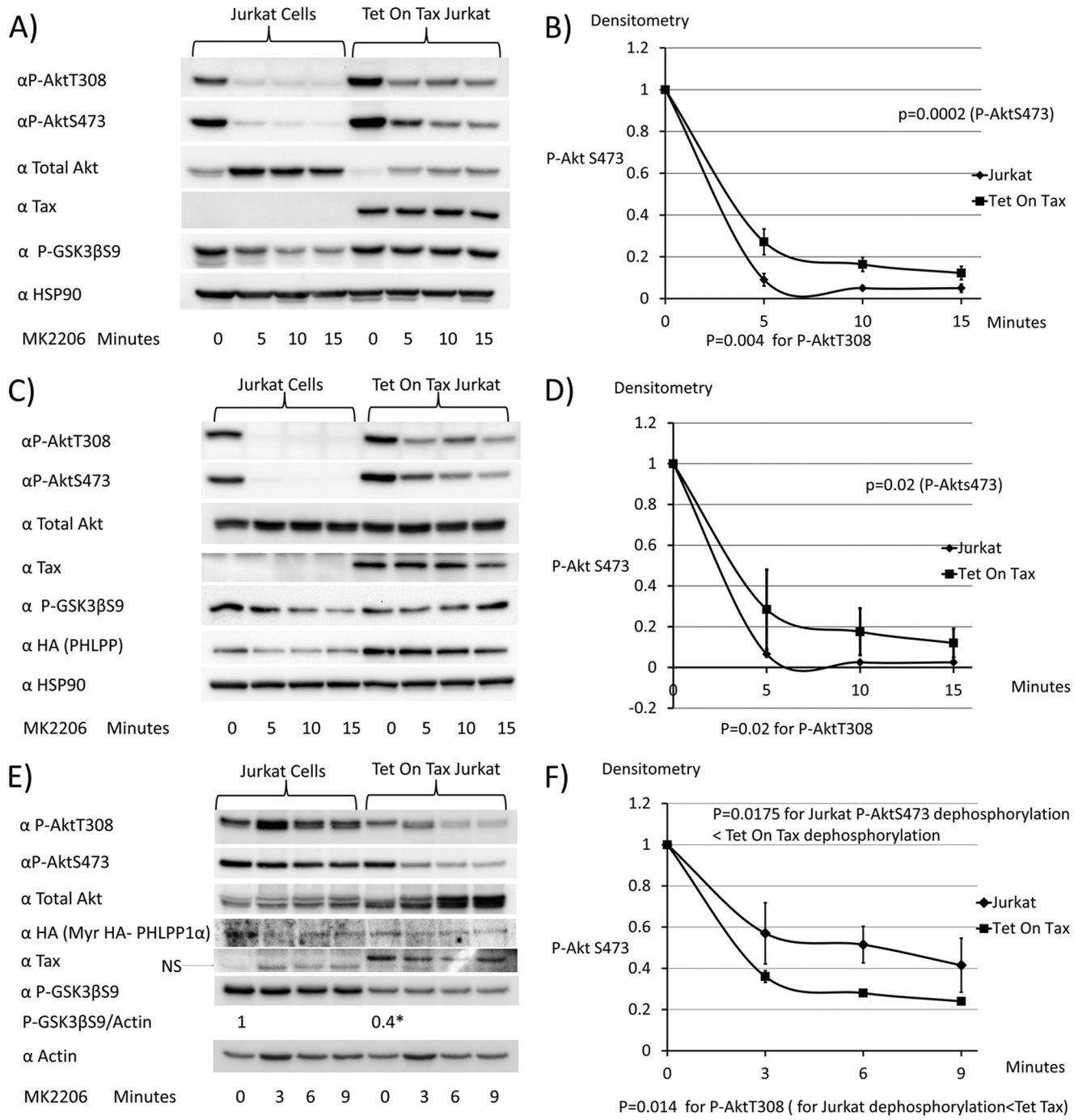

FIGURE 8. **Expression of membrane-associated PHLPP overcomes the effects of Tax1 on rates of Akt dephosphorylation.** *A* and *B*, Jurkat cells and Tet-On Tax1 Jurkat cells maintained in doxycycline for 48 h were treated with the Akt inhibitor MK2206, and samples were taken at serial time points to assess levels of P-AktThr-308(*P-AktT308*), P-AktSer-473 (*P-AktS473*), total Akt, Tax1, P-GSK3β Ser-9 (*P-GSK3βS9*), and HSP90. The levels of P-AktSer-473 at each time point were normalized to values obtained at 0 min of MK2206 treatment. *C* and *D*, doxycycline-treated Jurkat cells and Tet on Tax1 Jurkat cells were transiently transfected with a PHLPP expression vector for $6^1/_2$ h and then treated with MK2206, and samples were taken at serial time points to compare Akt dephosphorylation rates, as described above. *E* and *F*, doxycycline-treated Jurkat cells and Tet-On Tax1 Jurkat cells were transfected with a myristoylated PHLPP expression plasmid for $6^1/_2$ h and then treated with MK2206, and samples were taken at serial time points to compare Akt dephosphorylation rates, as described above. Dephosphorylation curves were generated from two independent experiments. The baseline P-AktSer-473 level is normalized to 1 for dephosphorylation curves.

To demonstrate lack of competition of Tax2 for binding of PTEN to DLG1 immunoprecipitates with control IgG and anti-GFP using lysates of 293T cells expressing DLG1(GFP-DLG1), PTEN(HA-PTEN), and either Tax1(STax1) or Tax2(STax2) were performed (Fig. 9*B*). Immunoblot for Stag of DLG1 immunoprecipitates demonstrates interaction of Tax1 but not of Tax2 with DLG1 (Fig. 9*B*, *upper panel, lane 4 versus 5*). Expression of Tax1 with PTEN demonstrated less PTEN associated with DLG-1 than in the absence of Tax1 (Fig. 9*B*, *lane 4 versus 3*). Expression of Tax2 with PTEN resulted in higher levels of PTEN in complex with DLG-1 than with expression of Tax1 (Fig. 9*B*, *lane 5 versus 4*) and similar levels of PTEN associated with DLG-1 to that seen in the absence of Tax1 (Fig. 9*B*, *lanes 5 versus 3*). Immunoblots of total lysates for HA-PTEN,

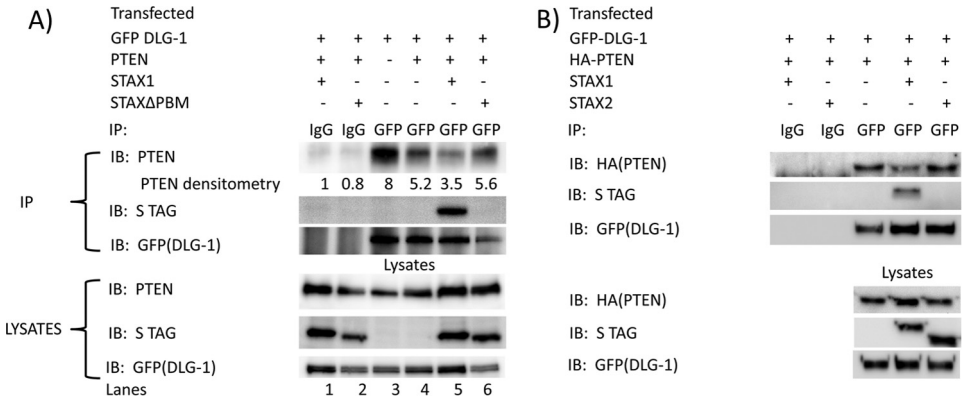

FIGURE 9. **Tax competes with PTEN for interaction with DLG-1.** *A,* 293T cells were co-transfected with expression plasmids for GFP-DLG-1, PTEN, and either S-tagged HTLV1 Tax or S-tagged C-terminal PBM deletion mutant of Tax for 48 h. Cell lysates were immunoprecipitated with control goat IgG or goat anti-GFP. Cell lysates and immunoprecipitates were examined by immunoblot performed with antibodies to PTEN, Tax (STag), and DLG-1 (GFP). Similar results were obtained in two independent experiments. *B,* 293T cells were co-transfected with expression plasmids for GFP-DLG-1, PTEN, and either S-tagged HTLV1 Tax or S-tagged HTLV2 Tax for 48 h. Cell lysates were immunoprecipitated with control goat IgG or goat anti-GFP. Cell lysates and immunoprecipitates were examined by immunoblot performed with antibodies to PTEN (HA), Tax (S tag), and DLG-1 (GFP). Similar results were obtained in two independent experiments.

STag, and GFP-DLG-1 confirmed the expression of these proteins (Fig. 9*B*, *bottom three panels*). These findings are consistent with the hypothesis that Tax1 competes with PTEN for interaction with DLG-1, through its PDZ-binding motif.

Discussion

Tax1 has significantly greater transformation potential than Tax2 in various experimental contexts (10–13, 17). In addition, although HTLV-1 is a leukemogenic virus, which causes a rapidly progressive T-cell leukemia/lymphoma in humans, HTLV-2 causes no human disease. Tax1 and Tax2 induce canonical NFκB equally, but Tax1, unlike Tax2, activates the non-canonical NFκB pathway, an observation confirmed in this study (10, 17).

Previous studies into the differences between these homologous proteins revealed that loss of either of two critical regions of Tax1, LZ or PBM, reduced transformation potential (17). Moreover, switching the LZ region of Tax1 with the corresponding region of Tax2 results in attenuated non-canonical NFκB activation. When we compared the leucine zipper mutant to wild-type Tax1, we also found attenuated p100 processing.

Previous work also suggested that deletion of the C-terminal PBM of Tax1 leads to attenuated non-canonical NFκB activation (12). However, when we compared Tax1 and the Tax1ΔPBM mutant, we saw higher levels of p100 processing induced by the mutant. It is possible that this difference is due to different methodology for expressing Tax1 proteins. In the earlier publication (12), stable transduction of cells with Tax1-expressing retrovirus was used, and the cells were subjected to drug selection. In certain contexts, for example, the absence of simultaneous GSK3β inhibition, there may a viability cost to non-canonical NFκB activation, and p52 may behave like a tumor suppressor in this context (41–44). It is therefore possible that in the absence of simultaneous Akt activation, p100 processing may be lost during cell passaging required for drug selection. Because we did not see a difference in non-canonical NFκB activation by Tax1ΔPBM, the attenuated transformation potential of the Tax1ΔPBM mutant remained to be explained.

We focused on the potential functions of the Tax1 PBM. Previous data showed that Tax1 PBM interacted with PDZ domain scaffolding proteins DLG-1, hScrib, MAGI-1, and MAGI-3 (25–28). We performed mass spectrometric analyses of Tax1, Tax2, and Tax1ΔPBM immunoprecipitates, which confirmed the interaction of Tax1, but not Tax2 or Tax1ΔPBM, with DLG-1.

We noted that the same PDZ domain proteins bound the tumor suppressors PTEN and PHLPP, which are key phosphatases in the PI3K-Akt-mTOR pathway (20–23, 45). We therefore hypothesized that Tax1, but not Tax1ΔPBM, may activate the PI3K-Akt-mTOR pathway by mislocalizing the tumor suppressors PTEN and PHLPP from the plasma membrane, thereby negatively regulating their activity. We confirmed that Akt is activated in HTLV-transformed cell lines. We also found that Tax1 expression causes Akt activation, whereas Tax1ΔPBM and Tax2 lack this function.

This study demonstrates that effects of Tax1 on PTEN and PHLPP are at least partially responsible for Akt activation. The effects of Tax1 on PTEN and PHLPP occurred at a post-translational step. Forced membrane localization of either PTEN or PHLPP overcame the negative influence of Tax1 on their phosphatase activity for PI3K and Akt, respectively. In these experiments, the kinetics of dephosphorylation of Akt was measured under conditions where upstream signals were abrogated with a PI3K or Akt inhibitor, respectively. With forced membrane expression of PTEN, rates of Akt dephosphorylation in the presence or absence of Tax1 were similar. Forced membrane expression of PHLPP resulted in rates of Akt dephosphorylation that were actually higher in Tax1-expressing cells than control cells. Although the explanation for this finding is unclear, we conjecture that there may be compensatory mechanisms for the increased state of Akt activation in Tax1-expressing cells, such as Akt-mediated suppression of Forkhead box O-induced transcription of *Rictor* and *Sestrin3* genes, whose products increase AktSer-473 phosphorylation (46).

Our studies suggest that Tax1 may activate the PI3K-Akt-mTOR pathway by antagonizing the activity of PTEN and

PHLPP. Co-immunoprecipitation assays demonstrated that Tax1, but not Tax1ΔPBM or Tax2, competes with PTEN for binding to DLG-1. Thus, inhibition of PTEN and PHLPP binding to PDZ proteins is a likely mechanism for these effects. Previous studies suggested that Tax1 expression may lead to mislocalization of PDZ proteins (26, 47). This may represent an additional mechanism for the displacement of PTEN and PHLPP from the plasma membrane.

The current and previous studies showed that Tax1 binds multiple PDZ-containing proteins, including DLG-1, hScrib, and MAGI that could modulate Akt activity. Other PDZ-containing proteins may also have a similar activity. Although Tax1 competes with DLG-1 binding to PTEN, inhibition of binding to PTEN was incomplete (Fig. 9). Furthermore, RNA interference with either DLG1 or hScrib failed to overcome the effects of Tax1 on Akt phosphorylation (data not shown). In contrast, simultaneous knockdown of multiple PDZ-containing proteins might overcome the effects of Tax1.

Akt is activated in HTLV-1 transformed cell lines and ATL cells (48, 49). This suggests a role for PI3K and Akt inhibitors for treatment of ATL. The human papilloma virus E6 protein also possesses a C-terminal PBM that shares many binding partners with HTLV-1 Tax (50–53). Given the role of E6 in many squamous cell carcinomas of the head and neck, anal canal, and uterine cervix, the role of PI3K activation in these malignancies warrants further investigation, especially given the potential therapeutic implications (54).

Author Contributions—M. C. and L. R. conceived the experiments; M. C., H. B., J. A.-S., N. S., and M. K. performed the experiments; and P. G. provided critical reagents. All authors revised and approved the manuscript.

References

1. Gallo, R. C. (2005) The discovery of the first human retrovirus: HTLV-1 and HTLV-2. *Retrovirology* **2,** 17
2. Poiesz, B. J., Ruscetti, F. W., Reitz, M. S., Kalyanaraman, V. S., and Gallo, R. C. (1981) Isolation of a new type C retrovirus (HTLV) in primary uncultured cells of a patient with Sezary T-cell leukaemia. *Nature* **294,** 268–271
3. Grassmann, R., Berchtold, S., Radant, I., Alt, M., Fleckenstein, B., Sodroski, J. G., Haseltine, W. A., and Ramstedt, U. (1992) Role of human T-cell leukemia virus type 1 X region proteins in immortalization of primary human lymphocytes in culture. *J. Virol.* **66,** 4570–4575
4. Tanaka, A., Takahashi, C., Yamaoka, S., Nosaka, T., Maki, M., and Hatanaka, M. (1990) Oncogenic transformation by the tax gene of human T-cell leukemia virus type I *in vitro*. *Proc. Natl. Acad. Sci. U.S.A.* **87,** 1071–1075
5. Grossman, W. J., Kimata, J. T., Wong, F. H., Zutter, M., Ley, T. J., and Ratner, L. (1995) Development of leukemia in mice transgenic for the tax gene of human T-cell leukemia virus type I. *Proc. Natl. Acad. Sci. U.S.A.* **92,** 1057–1061
6. Akagi, T., Ono, H., Nyunoya, H., and Shimotohno, K. (1997) Characterization of peripheral blood T-lymphocytes transduced with HTLV-I Tax mutants with different trans-activating phenotypes. *Oncogene* **14,** 2071–2078
7. Currer, R., Van Duyne, R., Jaworski, E., Guendel, I., Sampey, G., Das, R., Narayanan, A., and Kashanchi, F. (2012) HTLV tax: a fascinating multifunctional co-regulator of viral and cellular pathways. *Front. Microbiol.* **3,** 406
8. Robek, M. D., and Ratner, L. (1999) Immortalization of $CD4^+$ and $CD8^+$ T lymphocytes by human T-cell leukemia virus type 1 Tax mutants expressed in a functional molecular clone. *J. Virol.* **73,** 4856–4865
9. Feuer, G., and Green, P. L. (2005) Comparative biology of human T-cell lymphotropic virus type 1 (HTLV-1) and HTLV-2. *Oncogene* **24,** 5996–6004
10. Endo, K., Hirata, A., Iwai, K., Sakurai, M., Fukushi, M., Oie, M., Higuchi, M., Hall, W. W., Gejyo, F., and Fujii, M. (2002) Human T-cell leukemia virus type 2 (HTLV-2) Tax protein transforms a rat fibroblast cell line but less efficiently than HTLV-1 Tax. *J. Virol.* **76,** 2648–2653
11. Tsubata, C., Higuchi, M., Takahashi, M., Oie, M., Tanaka, Y., Gejyo, F., and Fujii, M. (2005) PDZ domain-binding motif of human T-cell leukemia virus type 1 Tax oncoprotein is essential for the interleukin 2 independent growth induction of a T-cell line. *Retrovirology* **2,** 46
12. Higuchi, M., Tsubata, C., Kondo, R., Yoshida, S., Takahashi, M., Oie, M., Tanaka, Y., Mahieux, R., Matsuoka, M., and Fujii, M. (2007) Cooperation of NF-κB2/p100 activation and the PDZ domain-binding motif signal in human T-cell leukemia virus type 1 (HTLV-1) Tax1 but not HTLV-2 Tax2 is crucial for interleukin-2-independent growth transformation of a T-cell line. *J. Virol.* **81,** 11900–11907
13. Shoji, T., Higuchi, M., Kondo, R., Takahashi, M., Oie, M., Tanaka, Y., Aoyagi, Y., and Fujii, M. (2009) Identification of a novel motif responsible for the distinctive transforming activity of human T-cell leukemia virus (HTLV) type 1 Tax1 protein from HTLV-2 Tax2. *Retrovirology* **6,** 83
14. Ren, T., and Cheng, H. (2013) Differential transforming activity of the retroviral Tax oncoproteins in human T lymphocytes. *Front. Microbiol.* **4,** 287
15. Ciminale, V., Rende, F., Bertazzoni, U., and Romanelli, M. G. (2014) HTLV-1 and HTLV-2: highly similar viruses with distinct oncogenic properties. *Front. Microbiol.* **5,** 398
16. Romanelli, M. G., Diani, E., Bergamo, E., Casoli, C., Ciminale, V., Bex, F., and Bertazzoni, U. (2013) Highlights on distinctive structural and functional properties of HTLV Tax proteins. *Front. Microbiol.* **4,** 271
17. Higuchi, M., and Fujii, M. (2009) Distinct functions of HTLV-1 Tax1 from HTLV-2 Tax2 contribute key roles to viral pathogenesis. *Retrovirology* **6,** 117
18. Xiao, G., Cvijic, M. E., Fong, A., Harhaj, E. W., Uhlik, M. T., Waterfield, M., and Sun, S.-C. (2001) Retroviral oncoprotein Tax induces processing of NF-κB2/p100 in T-cells: evidence for the involvement of IKKα. *EMBO J.* **20,** 6805–6815
19. Molina, J. R., Agarwal, N. K., Morales, F. C., Hayashi, Y., Aldape, K. D., Cote, G., and Georgescu, M. M. (2012) PTEN, NHERF1 and PHLPP form a tumor suppressor network that is disabled in glioblastoma. *Oncogene* **31,** 1264–1274
20. Li, X., Yang, H., Liu, J., Schmidt, M. D., and Gao, T. (2011) Scribble-mediated membrane targeting of PHLPP1 is required for its negative regulation of Akt. *EMBO Rep.* **12,** 818–824
21. Sotelo, N. S., Valiente, M., Gil, A., and Pulido, R. (2012) A functional network of the tumor suppressors APC, hDlg, and PTEN that relies on recognition of specific PDZ-domains. *J. Cell. Biochem.* **113,** 2661–2670
22. Wu, X., Hepner, K., Castelino-Prabhu, S., Do, D., Kaye, M. B., Yuan, X. J., Wood, J., Ross, C., Sawyers, C. L., and Whang, Y. E. (2000) Evidence for regulation of the PTEN tumor suppressor by a membrane-localized multi-PDZ domain containing scaffold protein MAGI-2. *Proc. Natl. Acad. Sci. U.S.A.* **97,** 4233–4238
23. Adey, N. B., Huang, L., Ormonde, P. A., Baumgard, M. L., Pero, R., Byreddy, D. V., Tavtigian, S. V., and Bartel, P. L. (2000) Threonine phosphorylation of the MMAC1/PTEN PDZ-binding domain both inhibits and stimulates PDZ binding. *Cancer Res.* **60,** 35–37
24. Gao, T., Furnari, F., and Newton, A. C. (2005) PHLPP: a phosphatase that directly dephosphorylates Akt, promotes apoptosis, and suppresses tumor growth. *Mol. Cell* **18,** 13–24
25. Suzuki, T., Ohsugi, Y., Uchida-Toita, M., Akiyama, T., and Yoshida, M. (1999) Tax oncoprotein of HTLV-1 binds to the human homologue of *Drosophila* discs large tumor suppressor protein, hDLG, and perturbs its function in cell growth control. *Oncogene* **18,** 5967–5972
26. Okajima, M., Takahashi, M., Higuchi, M., Ohsawa, T., Yoshida, S., Yoshida, Y., Oie, M., Tanaka, Y., Gejyo, F., and Fujii, M. (2008) Human T-cell leukemia virus type 1 Tax induces an aberrant clustering of the tumor

suppressor Scribble through the PDZ domain-binding motif dependent and independent interaction. *Virus Genes* **37,** 231–240
27. Ohashi, M., Sakurai, M., Higuchi, M., Mori, N., Fukushi, M., Oie, M., Coffey, R. J., Yoshiura, K., Tanaka, Y., Uchiyama, M., Hatanaka, M., and Fujii, M. (2004) Human T-cell leukemia virus type 1 Tax oncoprotein induces and interacts with a multi-PDZ domain protein, MAGI-3. *Virology* **320,** 52–62
28. Makokha, G. N., Takahashi, M., Higuchi, M., Saito, S., Tanaka, Y., and Fujii, M. (2013) Human T-cell leukemia virus type 1 Tax protein interacts with and mislocalizes the PDZ domain protein MAGI-1. *Cancer Sci.* **104,** 313–320
29. Kwon, H., Ogle, L., Benitez, B., Bohuslav, J., Montano, M., Felsher, D. W., and Greene, W. C. (2005) Lethal cutaneous disease in transgenic mice conditionally expressing type I human T-cell leukemia virus Tax. *J. Biol. Chem.* **280,** 35713–35722
30. Ramaswamy, S., Nakamura, N., Vazquez, F., Batt, D. B., Perera, S., Roberts, T. M., and Sellers, W. R. (1999) Regulation of G1 progression by the PTEN tumor suppressor protein is linked to inhibition of the phosphatidylinositol 3-kinase/Akt pathway. *Proc. Natl. Acad. Sci. U.S.A.* **96,** 2110–2115
31. Leslie, N. R., Bennett, D., Gray, A., Pass, I., Hoang-Xuan, K., and Downes, C. P. (2001) Targeting mutants of PTEN reveal distinct subsets of tumour suppressor functions. *Biochem. J.* **357,** 427–435
32. Lin, E. I., Jeyifous, O., and Green, W. N. (2013) CASK regulates SAP97 conformation and its interactions with AMPA and NMDA receptors. *J. Neurosci.* **33,** 12067–12076
33. Smith, P. K., Krohn, R. I., Hermanson, G. T., Mallia, A. K., Gartner, F. H., Provenzano, M. D., Fujimoto, E. K., Goeke, N. M., Olson, B. J., and Klenk, D. C. (1985) Measurement of protein using bicinchoninic acid. *Anal. Biochem.* **150,** 76–85
34. Ornstein, L. (1964) Disc electrophoresis. I. background and theory. *Ann. N.Y. Acad. Sci.* **121,** 321–349
35. Laemmli, U. K. (1970) Cleavage of structural proteins during the assembly of the head of bacteriophage T4. *Nature* **227,** 680–685
36. Dissinger, N., Shkriabai, N., Hess, S., Al-Saleem, J., Kvaratskhelia, M., and Green, P. L. (2014) Identification and characterization of HTLV-1 HBZ post-translational modifications. *PLoS One* **9,** e112762
37. Xie, L., Yamamoto, B., Haoudi, A., Semmes, O. J., and Green, P. L. (2006) PDZ binding motif of HTLV-1 Tax promotes virus-mediated T-cell proliferation *in vitro* and persistence *in vivo*. *Blood* **107,** 1980–1988
38. Wu, Y. T., Ouyang, W., Lazorchak, A. S., Liu, D., Shen, H. M., and Su, B. (2011) mTOR complex 2 targets Akt for proteasomal degradation via phosphorylation at the hydrophobic motif. *J. Biol. Chem.* **286,** 14190–14198
39. Adachi, M., Katsumura, K. R., Fujii, K., Kobayashi, S., Aoki, H., and Matsuzaki, M. (2003) Proteasome-dependent decrease in Akt by growth factors in vascular smooth muscle cells. *FEBS Lett.* **554,** 77–80
40. Comb, W. C., Hutti, J. E., Cogswell, P., Cantley, L. C., and Baldwin, A. S. (2012) p85α SH2 domain phosphorylation by IKK promotes feedback inhibition of PI3K and Akt in response to cellular starvation. *Mol. Cell* **45,** 719–730
41. Rocha, S., Martin, A. M., Meek, D. W., and Perkins, N. D. (2003) p53 represses cyclin D1 transcription through down regulation of Bcl-3 and inducing increased association of the p52 NF-κB subunit with histone deacetylase 1. *Mol. Cell. Biol.* **23,** 4713–4727
42. Schumm, K., Rocha, S., Caamano, J., and Perkins, N. D. (2006) Regulation of p53 tumour suppressor target gene expression by the p52 NF-κB subunit. *EMBO J.* **25,** 4820–4832
43. Barré, B., Coqueret, O., and Perkins, N. D. (2010) Regulation of activity and function of the p52 NF-κB subunit following DNA damage. *Cell Cycle* **9,** 4795–4804
44. Barré, B., and Perkins, N. D. (2010) The Skp2 promoter integrates signaling through the NF-κB, p53, and Akt/GSK3β pathways to regulate autophagy and apoptosis. *Mol. Cell* **38,** 524–538
45. Wu, Y., Dowbenko, D., Spencer, S., Laura, R., Lee, J., Gu, Q., and Lasky, L. A. (2000) Interaction of the tumor suppressor PTEN/MMAC with a PDZ domain of MAGI3, a novel membrane-associated guanylate kinase. *J. Biol. Chem.* **275,** 21477–21485
46. Chen, C. C., Jeon, S. M., Bhaskar, P. T., Nogueira, V., Sundararajan, D., Tonic, I., Park, Y., and Hay, N. (2010) FoxOs inhibit mTORC1 and activate Akt by inducing the expression of Sestrin3 and Rictor. *Dev. Cell* **18,** 592–604
47. Arpin-André, C., and Mesnard, J. M. (2007) The PDZ domain-binding motif of the human T-cell leukemia virus type 1 tax protein induces mislocalization of the tumor suppressor hScrib in T-cells. *J. Biol. Chem.* **282,** 33132–33141
48. Peloponese, J. M., Jr., and Jeang, K. T. (2006) Role for Akt/protein kinase B and activator protein-1 in cellular proliferation induced by the human T-cell leukemia virus type 1 tax oncoprotein. *J. Biol. Chem.* **281,** 8927–8938
49. Fukuda, R., Hayashi, A., Utsunomiya, A., Nukada, Y., Fukui, R., Itoh, K., Tezuka, K., Ohashi, K., Mizuno, K., Sakamoto, M., Hamanoue, M., and Tsuji, T. (2005) Alteration of phosphatidylinositol 3-kinase cascade in the multilobulated nuclear formation of adult T-cell leukemia/lymphoma (ATLL). *Proc. Natl. Acad. Sci. U.S.A.* **102,** 15213–15218
50. Lee, S. S., Weiss, R. S., and Javier, R. T. (1997) Binding of human virus oncoproteins to hDlg/SAP97, a mammalian homolog of the *Drosophila* discs large tumor suppressor protein. *Proc. Natl. Acad. Sci. U.S.A.* **94,** 6670–6675
51. Kiyono, T., Hiraiwa, A., Fujita, M., Hayashi, Y., Akiyama, T., and Ishibashi, M. (1997) Binding of high-risk human papillomavirus E6 oncoproteins to the human homologue of the *Drosophila* discs large tumor suppressor protein. *Proc. Natl. Acad. Sci. U.S.A.* **94,** 11612–11616
52. Nakagawa, S., and Huibregtse, J. M. (2000) Human scribble (Vartul) is targeted for ubiquitin-mediated degradation by the high-risk papillomavirus E6 proteins and the E6AP ubiquitin-protein ligase. *Mol. Cell. Biol.* **20,** 8244–8253
53. Grm, H. S., and Banks, L. (2004) Degradation of hDlg and MAGIs by human papillomavirus E6 is E6-AP-independent. *J. Gen. Virol.* **85,** 2815–2819
54. Contreras-Paredes, A., De la Cruz-Hernández, E., Martínez-Ramírez, I., Dueñas-González, A., and Lizano, M. (2009) E6 variants of human papillomavirus 18 differentially modulate the protein kinase B/phosphatidylinositol 3-kinase (akt/PI3K) signaling pathway. *Virology* **383,** 78–85